THE JOURNAL OF COMPARATIVE NEUROLOGY 366:717–725 (1996)

Mapping of the Basal Forebrain Cholinergic System of the Dog: A Choline Acetyltransferase Immunohistochemical Study

RENÉ ST-JACQUES, WOJCIECH GORCZYCA, GÉRARD MOHR, AND HYMAN M. SCHIPPER

Department of Neurology and Neurosurgery (G.M., H.M.S.), Lady Davis Institute for Medical Research (R.St-J., W.G., G.M. and H.M.S.), and Bloomfield Center for Research in Aging (H.M.S.), Sir Mortimer B. Davis-Jewish General Hospital, McGill University, Montréal, Québec, Canada H3T 1E2

ABSTRACT

In an effort to produce a canine model of basal forebrain ischemia with memory deficits, we have shown that dogs possess a medial striate artery that perfuses basal forebrain territory, homologous to the human recurrent artery of Heubner. In the present study, we set out to delineate the precise topography of the cholinergic neurons in the canine forebrain, a neuronal system implicated in cognitive and memory functions. Floating coronal sections, derived from the head of the caudate nucleus to the rostral border of the hippocampus, were stained for choline acetyltransferase using a monoclonal antibody. Representative sections from one dog brain were drawn. These outlines were used for measurement of cell density, cell size, number of processes, and cell roundness. Choline acetyltransferase-positive neurons constituted four major subdivisions within the basal forebrain. A relatively dense population of cholinergic neurons was present in the medial septal nucleus (Ch1). A continuum of densely packed cells was also delineated within the vertical (Ch2) and horizontal (Ch3) nuclei of the diagonal band of Broca. A fourth group of heterogeneously packed cholinergic neurons represented the nucleus basalis magnocellularis (Ch4). Except for the caudal component of the Ch4 population, the forebrain cholinergic corticopetal system was located within the perfusion territory of the medial striate arteries. The Ch4 cell group in dogs is better defined than that of rodents but is not as sharply demarcated as in human and nonhuman primates. Our findings indicate that the dog may serve as an excellent model for assessing neurological and memory deficits, which, in humans, results from hypoperfusion of the recurrent artery of Heubner.

Indexing terms: memory, cholinergic neurons, nucleus basalis, ischemia

A number of studies have indicated that hypoperfusion in the territory of the recurrent artery of Heubner (RAH) in humans may result in cognitive deficits (Sweet et al., 1966; Talland et al., 1967; Gade, 1982; Volpe and Hirst, 1983; Vilkki, 1985; Larsson et al., 1989; Caplan et al., 1990; Yanagihara, 1991; Ries et al., 1993). The RAH has been shown to perfuse a well-defined territory which includes the head of the caudate nucleus, the anterior limb of the internal capsule, the substantia innominata, and the horizontal nucleus of the diagonal band of Broca (Gorczyca and Mohr, 1987).

An animal model of cognitive/memory deficits resulting from RAH hypoperfusion is not yet available. The relatively large brain volume and caliber of cerebral vessels in dogs may render these animals ideally suited for modeling human cerebrovascular ischemia within discrete perfusion territories of individual arteries. In a recent study (St-Jacques et al., 1993), we showed that the dog possesses a medial striate artery (MSA) homologous, according to its perfusion territory, to the human RAH. This perfusion territory includes an area corresponding to the nucleus basalis of Meynert (NbM; nucleus basalis magnocellularis in animals). In humans, this structure contains cholinergic neurons implicated in normal cognitive/memory function and the pathogenesis of Alzheimer's disease (AD).

Accepted October 13, 1995.

Address reprint requests to Dr. Gérard Mohr, Sir Mortimer B. Davis-Jewish General Hospital, Division of Neurosurgery, 3755 Côte Ste-Catherine Rd., Montréal, Québec, Canada, H3T 1E2.

From the comparative study of Gorry (1963), it is known that the ontogenesis of the NbM as a discrete magnocellular nucleus in mammals is proportional to the phylogenetic evolution of the species (rodent < canine < monkey < cetacean and human). Unfortunately, choline acetyltransferase (CLAT) was not available at that time, nor was it the intention of the author to provide a detailed map of the basal forebrain cholinergic system. Since then, only rats, cats, monkeys, and humans have had their basal forebrain cholinergic systems topographically delineated with any degree of precision.

As part of an effort to develop a canine model of basal forebrain focal ischemia with cognitive/memory deficits, we set out to map the basal forebrain cholinergic neurons in this species using ChAT immunohistochemistry.

MATERIALS AND METHODS

Subjects and tissue preparation

Five adult mongrel dogs of both sexes, weighing 24.6 ± 2.9 kg (mean± SD) were deeply anaesthetized with sodium pentobarbital (Somnotol; 50 mg/kg, i.v.). Brain fixation was achieved via perfusion of both common carotid arteries with 2 liters of ice-cold 0.9% heparinized saline followed by 1 liter of buffered 4% paraformaldehyde containing 15% v/v picric acid. The heads were immediately severed and kept overnight at 4°C. Brains were removed from the skull and kept at 4°C for 1–2 days in the paraformaldehyde solution and for an additional 24 hours in Tris buffer. A block of tissue containing the striatum was dissected out and sliced into 40-μm-thick coronal sections using a Vibratome (Lancer series 1000). Every tenth coronal section was selected for ChAT immunohistochemistry using adjacent sections as controls.

ChAT immunohistochemistry

Free-floating sections were incubated at room temperature for 20 minutes in 3% H_2O_2 to remove endogenous peroxidase activity followed by 30 minutes in 0.1% normal bovine serum. The sections were then incubated overnight at 4°C with a mouse monoclonal antibody against human ChAT (1-372-432; Boehringer Mannheim) at a working concentration of 3.3 μg/ml in bovine serum. Control sections were incubated without the primary antibody. On the following day the sections were immunohistochemically stained using the avidin-biotin complex technique (Vectastain ABC mouse kit; Vector Laboratories). The revelation medium consisted of 3,3′-diaminobenzidine (DAB) at 1 mg/ml with 0.1% H_2O_2 in Tris buffer. Tris buffer (Tris 0.1M; NaCl 0.15M at pH 7.4) was used as a rinsing solution between steps.

Abbreviations

AC	Anterior commissure
BSt	Bed nucleus of the stria terminalis
Caud	Caudate nucleus
ChAT	Choline acetyltransferase
Ch1	Cholinergic neurons of the medial septal area
Ch2	Cholinergic neurons of the vertical nucleus of the diagonal band of Broca
Ch3	Cholinergic neurons of the horizontal nucleus of the diagonal band of Broca
Ch4	Cholinergic neurons of the nucleus basalis magnocellularis
Ch4a	Anterior portion of the Ch4
Ch4id	Intermediodorsal portion of the Ch4
Ch4iv	Intermedioventral portion of the Ch4
Ch4p	Posterior portion of the Ch4
f	Fornix
GP	Globus pallidus
ICjM	Island of Cajal major
NbM	Nucleus basalis magnocellularis
OCh	Optic chiasm
Put	Putamen
RAH	Recurrent artery of Heubner
RT	Reticular thalamic nucleus
St	Stria terminalis

Coagulation factor VIII immunohistochemistry

In some animals, the sections were also stained for the von Willebrand's coagulation factor VIII to evaluate the relationship of ChAT-positive neurons to the microvasculature. The protocol was similar to that described above except that the primary antibody consisted of a rabbit polyclonal antiserum (1:100) against factor VIII (ABS000, Endotech), the secondary antibody was directed against rabbit immunoglobulin (Vectastain ABC rabbit kit; Vector Laboratories), and the chromogen was α-naphthol intensified with pyronin-B. This procedure selectively stains vascular endothelial cells.

The sections were floated onto slides, dried, and counterstained with methyl green (nuclear stain). One series of sections was also counterstained with cresyl violet (Nissl stain) to visualize total number of neurons (Fig. 1). After dehydration and clearing, the slides were coverslipped.

Mapping of ChAT-positive neurons

Eight sections of a brain were selected to construct an atlas of the basal forebrain area (Fig. 2). With the help of a drawing tube fixed to the microscope at low magnification (40×), outlines of the section perimeter, caudate nucleus, stria terminalis, putamen, globus pallidus, anterior commissure, ventricles, and cholinergic neurons were drawn.

Cellular density and morphometric measurements

Choline acetyltransferase-positive neuronal densities were evaluated at 100× magnification. Using the section crossing the level of the anterior commissure as reference (R = 25.0 from the atlas [Lim et al., 1960]), sections at approximate levels R27.8, R28.8, R24.6, and R22.2 as well as one section rostral and caudal to these were respectively chosen to evaluate the ChAT-positive neuronal density of the nucleus of the diagonal band of Broca (Ch2/3), medial septal area (Ch1), and nucleus basalis magnocellularis intermediodorsal and intermedioventral portions (Ch4id and Ch4iv) and posterior portion (Ch4p). In these sections, sampling was also performed for the caudate nucleus. Stained cells exhibiting nuclei were counted in each sampled area (Fig. 2). Cell density was expressed as number of cells per mm^2. According to West et al. (1991), we have evaluated the coefficient of error (CE) of the sampling scheme for each area in each individual, and compared these values with the coefficient of variation (CV) among individuals for each area. The obtained mean ratio, CE^2/CV^2, was approximately 0.25, indicating that the precision of the estimate obtained with our sampling scheme is most probably greater than that required for optimal sampling. Futhermore, for the purpose of comparison, total neuronal densities were evaluated in one animal in order to express ChAT positivity as percentage of total neurons per given region.

The collection of morphometric data was performed with the help of a video analysis software (JAVA v:1.3, Jandel

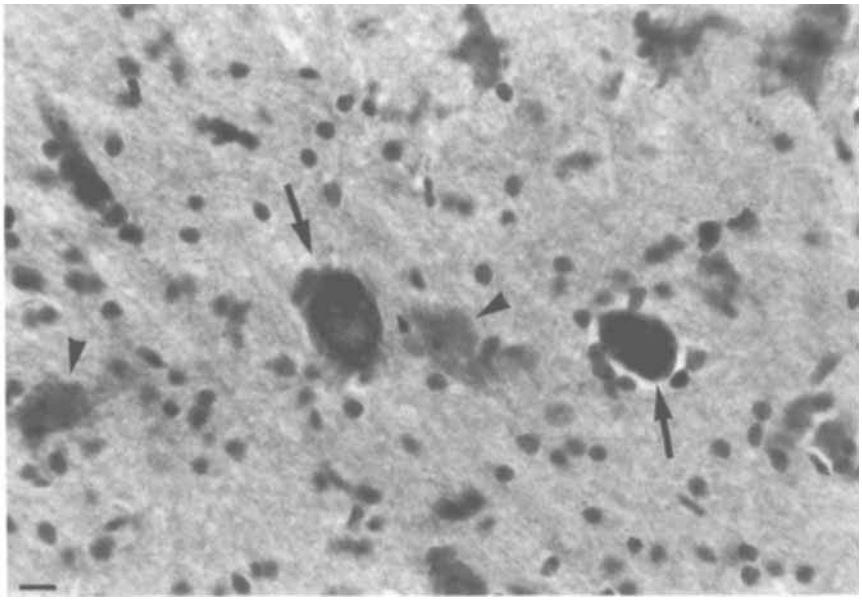

Fig. 1. Photomicrographs taken in the nucleus magnocellularis area showing ChAT-positive neurons counterstained with cresyl violet (Nissl stain). Arrowheads indicate magnocellular neurons not stained by ChAT, whereas arrows point to ChAT-positive magnocellular neurons. Scale bar is 15 μm.

Scientific) running on a 286 computer connected to a photomicroscope (KP-140, Hitachi and BH-2, Olympus). In each section, one field (300× final magnification) was randomly chosen and all ChAT-positive neurons in that field had their circumferences, cross-sectional areas, lengths, and widths measured. Cell roundness was computed according to the formula $4\pi A/C^2$, where A is the cross-sectional area in square microns and C is the circumference in microns. For a perfect circle, the roundness value equals 1.0. The number of processes per cell was also evaluated.

Statistics

Numerical data are expressed as mean ± SD. Comparisons between areas were made by using an ANOVA followed by Tukey's post hoc test with $P \leq 0.05$ indicating significance.

RESULTS

Specificity of ChAT staining

Choline acetyltransferase immunohistochemistry was highly specific with virtually no immunostaining observable in control preparations. ChAT immunoreactivity appeared as a diffuse brown reaction product within neuronal perikarya and proximal processes with sparing of the nucleus (Fig. 3).

Topography and morphology of ChAT-positive neurons

Choline acetyltransferase-positive neurons were found scattered throughout the striatum (Figs. 2A–H, 3A). They represent the least dense population of such neurons (Table 1). In the caudate nucleus, their size averaged 33.3 ± 10.1 by 16.1 ± 3.9 μm, and most of them were bipolar (Fig. 4).

In the internal capsule, ChAT-positive neurons were often arranged along the striatal cell bridges between the caudate nucleus and the putamen/globus pallidus (Fig. 3B).

ChAT-positive neurons of the medial septal area (Ch1) were located just dorsal and rostral to the decussation of the anterior commissure (Figs. 2C–E, 3C,D). Their size averaged 31.4 ± 7.1 by 16.9 ± 4.3 μm. These neurons were either mono- or bipolar (Fig. 4).

ChAT-positive neurons were also found in the vertical and horizontal nucleus of the diagonal band of Broca (Figs. 2B,C, 3 E,F). There was no clear delineation between these two groups (Ch2/3). Their sizes averaged 29.8 ± 6.7 by 18.3 ± 4.7 μm and 31.7 ± 7.6 by 18.2 ± 4.8 μm for the Ch2 and Ch3 cell groups, respectively. In Ch2, most of the cholinergic neurons were monopolar whereas in Ch3 they tended to be multipolar (Fig. 4).

The nucleus basalis magnocellularis (NbM-Ch4) is located just ventral to the globus-pallidus/putamen. Although not as sharply delineated as in primates, the Ch4 cell group in dogs can be divided into four subdivisions: anterior (Ch4a) (Fig. 2C,D); intermediodorsal (Ch4id) and intermedioventral (Ch4iv) (Fig. 2E– G); and posterior (Ch4p) (Figs. 2H, 3G). The latter subdivision represents the densest population of ChAT-positive neurons in the basal forebrain (Table 1). Most of the Ch4 cells were pyramidal in shape (Fig. 4) and measured 31.7 ± 6.5 by 17.9 ± 4.2 μm.

Comparisons between areas

Caudate cells were significantly smaller than Ch3 cells ($P < 0.05$; Table 2). Cell sizes did not differ significantly between any other regions examined ($P > 0.05$ for each comparison). Regarding cell roundness and number of processes, Ch1, Ch2, and Ch3 cells did not differ significantly from one another ($P > 0.05$ for each comparison), but cells in these subdivisions were significantly more

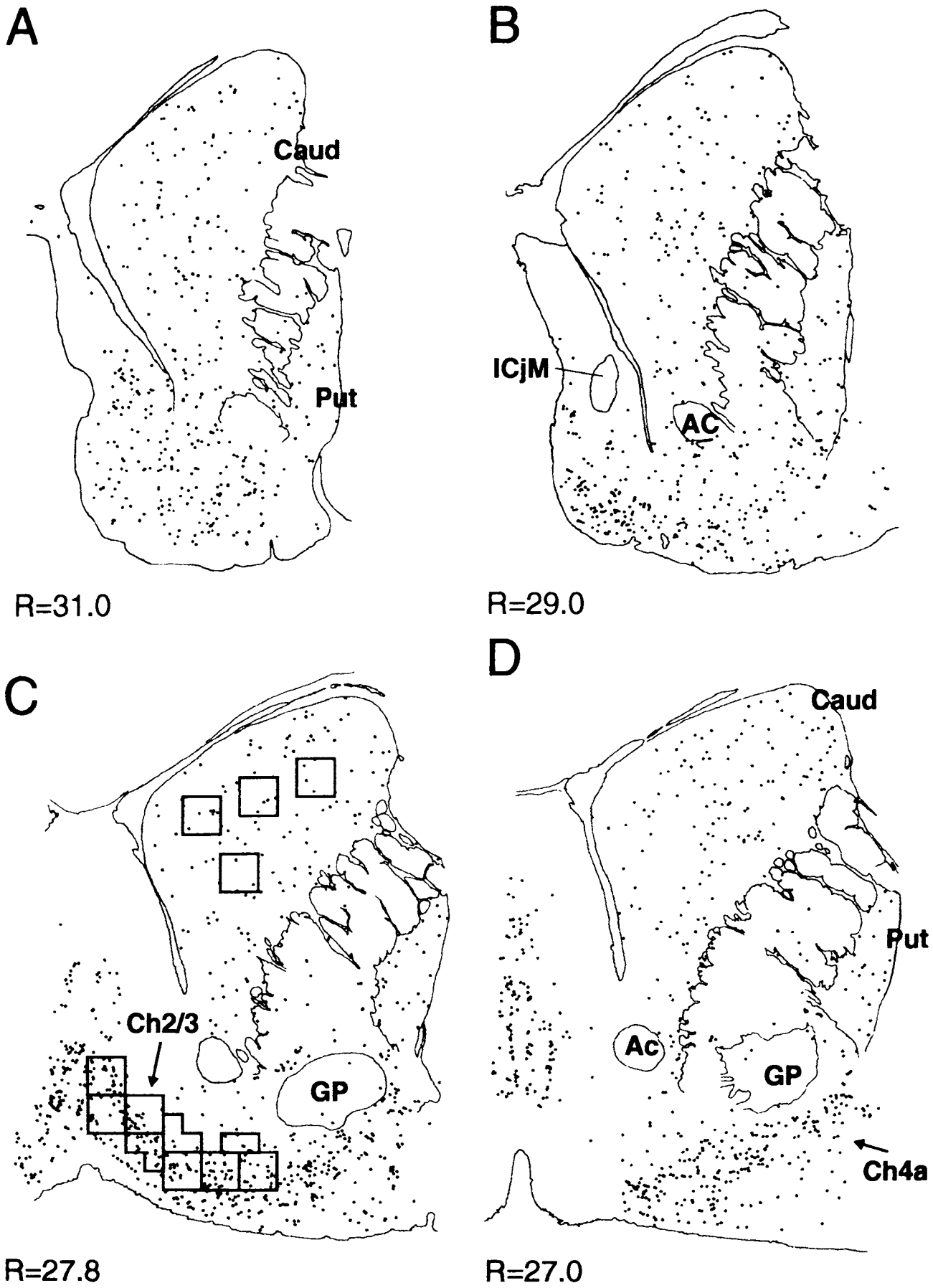

Fig. 2. Map of ChAT-positive neurons in the dog basal forebrain. Each dot represents a cholinergic neuron. 'R' refers to the levels of the sections according to the atlas of Mestre and Bons (1993). Squares denote areas sampled for cell density determination.

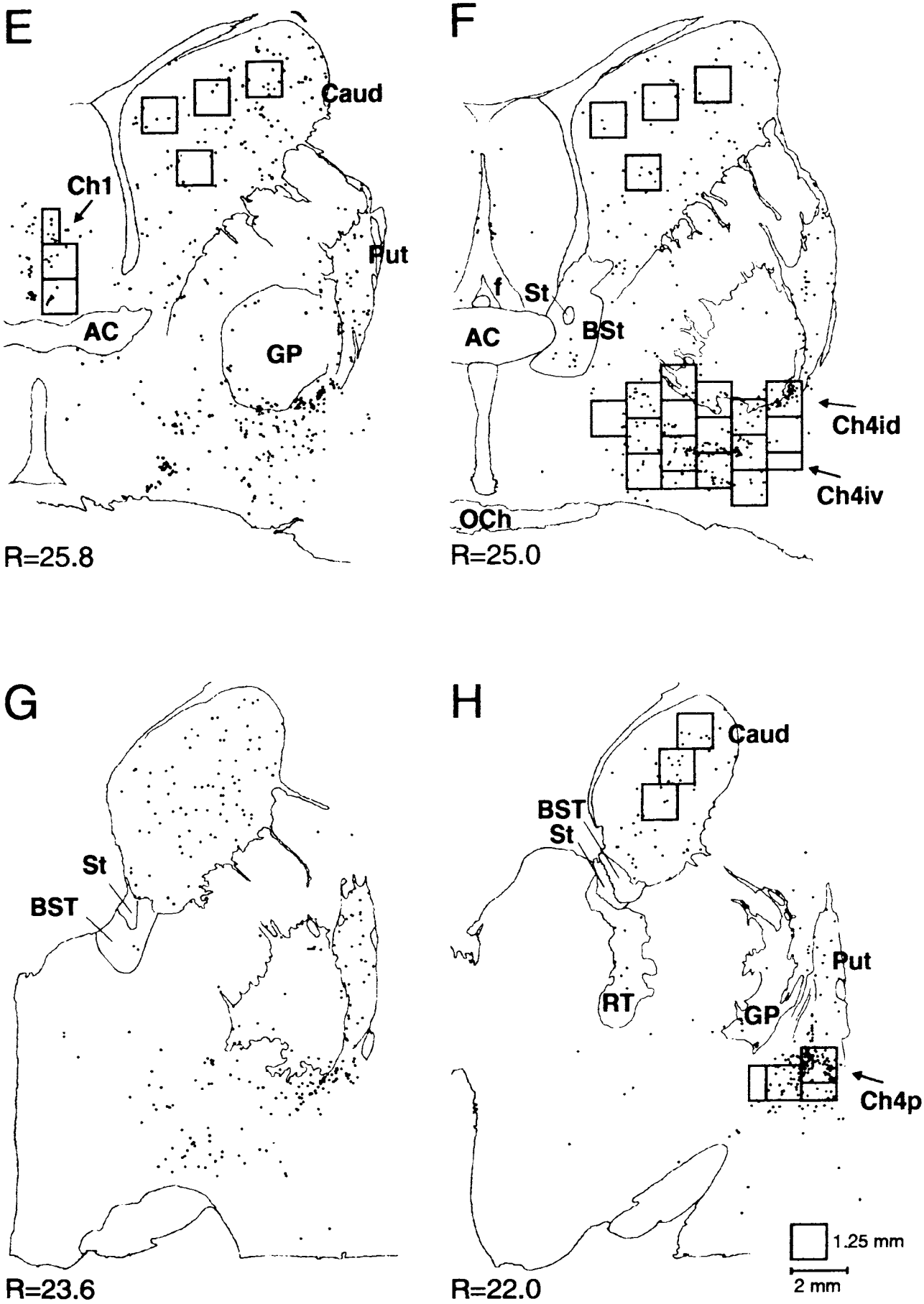

Fig. 2 Continued.

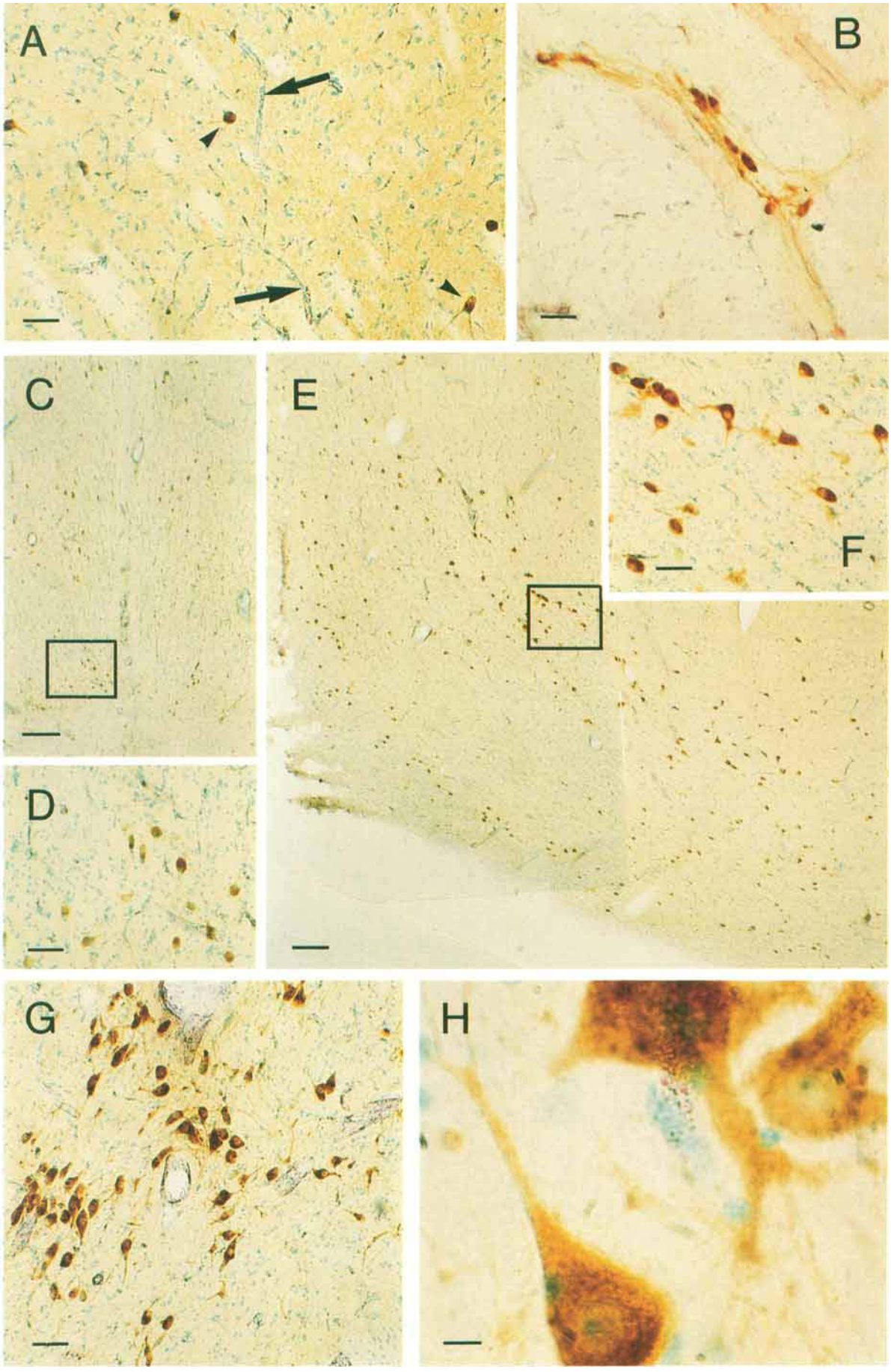

Figure 3

TABLE 1. Density of ChAT-Positive Neurons in the Dog's Basal Forebrain[1]

Areas	Side	Density of ChAT-neurons per mm² (each side and pooled)		Percentage of total (or magnocellular) neurons
Ch1	Right	12.4 ± 2.7	12.5 ± 2.0	6.8 ± 1.1
	Left	12.5 ± 1.5		
Ch2-3	Right	12.8 ± 2.9	12.9 ± 2.4	11.1 ± 2.1
	Left	12.9 ± 2.0		
Ch4id-iv	Right	8.8 ± 1.0	8.5 ± 0.9	5.6 ± 0.6 (34.3 ± 3.5)
	Left	8.2 ± 0.8		
Ch4p	Right	19.4 ± 4.3	18.8 ± 2.8	16.3 ± 2.4 (45.7 ± 6.7)
	Left	18.2 ± 3.3		
Caud	Right	2.8 ± 0.6	2.9 ± 0.6	0.4 ± 0.08
	Left	3.1 ± 0.7		

[1]Areas were defined in Figure 1. Data are expressed in cells/mm² as mean ± SD from five animals, both for the left and right hemispheres, and pooled for both sides. Total number of neurons has also been evaluated in one animal and the percentage of neurons that are ChAT-positive are presented.

TABLE 2. Morphological Differences Between ChAT-Positive Neurons of Different Areas[1]

Compared areas	Cross-sectional area	Roundness	No. of dendrites
Ch4 vs. Ch3	457 vs. 466	0.67 vs. 0.69*	2.35 vs. 1.95*
Ch4 vs. Ch2	457 vs. 445	0.67 vs. 0.72*	2.35 vs. 1.78*
Ch4 vs. Ch1	457 vs. 438	0.67 vs. 0.69*	2.35 vs. 1.78*
Ch4 vs. Caud	457 vs. 435	0.67 vs. 0.62*	2.35 vs. 2.12*
Ch3 vs. Ch2	466 vs. 445	0.69 vs. 0.72	1.95 vs. 1.78
Ch3 vs. Ch1	466 vs. 438	0.69 vs. 0.69	1.95 vs. 1.78
Ch3 vs. Caud	466 vs. 435*	0.69 vs. 0.62*	1.95 vs. 2.12
Ch2 vs. Ch1	445 vs. 438	0.72 vs. 0.69	1.78 vs. 1.78
Ch2 vs. Caud	445 vs. 435	0.72 vs. 0.62*	1.78 vs. 2.12*
Ch1 vs. Caud	438 vs. 435	0.69 vs. 0.62*	1.78 vs. 2.12*

[1]Cholinergic neurons in these regions are more readily differentiated on the basis of roundness and number of processes than overall size.
*Indicates significance at $P < 0.05$.

rounded and less often multipolar than cells in the caudate nucleus and Ch4 ($P < 0.05$ for each comparison).

Topographical relationship to the microvasculature

Generally, there was no apparent topographical relationship between ChAT-positive neurons and capillaries stained with anti-Factor VIII (Fig. 3), although Ch4 ChAT-positive neurons were occasionally found to encircle precapillaries (Fig. 3G).

DISCUSSION

This study provides, for the first time to our knowledge, a detailed map of the basal forebrain cholinergic system of the dog using ChAT-immunohistochemistry. As in the case of the rat (Armstrong et al., 1983), monkey (Mesulam et al., 1983), and human (Mesulam and Geula, 1988), cholinergic neurons in the forebrain of dogs were loosely scattered throughout the striatum and constituted a far more dense population in the medial septal area (Ch1), the vertical (Ch2), and horizontal (Ch3) nuclei of the diagonal band of Broca and within the nucleus basalis magnocellularis (Ch4) extending into the substantia innominata. Using Nissl-stained preparations, it was previously shown that the organization and complexity of the NbM increased with phylogenetic evolution (Gorry, 1963). In rats, subsectors are not readily defined for the Ch4 cell group (Armstrong et al., 1983) whereas in humans up to six subsectors can be delineated (Mesulam and Geula, 1988). In dogs, as in monkeys (Mesulam et al., 1983), we delineated four subsectors in the Ch4 cell group.

As part of an ongoing effort to produce a canine model of cholinergic deficits resulting from local basal forebrain ischemia, we confirmed that the Ch3/4 cell groups are located within the perfusion territory of the medial striate artery (St-Jacques et al., 1993). Only the most posterior portion of Ch4 seems to be outside that territory. If the projections of the Ch3/4 cell groups of the dog are comparable to those of other mammalian species, then ischemia in the territory of the medial striate artery is expected to affect cholinergic neurons projecting to the medial aspect of the cerebral hemispheres, to the frontoparietal, opercular, posterioparietal, inferotemporal, and peristriate areas, and to the amygdala and olfactory bulb. There is considerable evidence implicating these projections in a range of memory/cognitive functions (Mesulam, 1991). Thus, ischemia in the territory of the medial striate arteries in dogs is anticipated to produce neurobehavioural deficits homologous to those seen in humans following ischemic injury to forebrain structures perfused via Heubner's recurrent arteries. In humans, such injury arises clinically in the context of aneurysmal rupture or repair in the anterior circle of Willis (Sweet et al., 1966; Talland et al., 1967; Gade, 1982; Volpe and Hirst, 1983; Vilkki, 1985; Larsson et al., 1989).

In the present study, significant differences were observed between brain regions regarding not only the percentage of magnocellular neurons immunoreactive for ChAT, but also concerning sizes and morphologies of the cholinergic cells. These latter characteristics must be taken into account when assessing the effects of aging and disease on cholinergic populations in light of previous studies which demonstrated marked alterations in cholinergic dimensions and shape, but not number, following cortical injury and retrograde degeneration (Funnell et al., 1990; Garofalo and Cuello, 1994).

In conclusion, a map of ChAT-positive neurons in the basal forebrain of the dog is provided. Four subdivisions can be delineated for the Ch4 cell group in this species: anterior (Ch4a), intermediodorsal (Ch4id), intermedioventral (Ch4iv), and posterior (Ch4p). In dogs, cholinergic neurons within Ch3, Ch4a, Ch4id, and Ch4iv are situated within the perfusion territory of the medial striate artery which is homologous to the recurrent artery of Heubner in humans. Basal forebrain cholinergic deficiency resulting from experimental hypoperfusion of medial striate arteries in dogs may serve as a useful model for investigating the neurological deficits which accompany ischemia in the territory of Heubner's arteries in humans.

Fig. 3. Photomicrographs showing ChAT-positive neurons of the caudate nucleus (**A**), internal capsule (**B**), medial septal area (Ch1; **C** and **D**), vertical (Ch2) and horizontal (Ch3) nucleus of the diagonal band of Broca (**E** and **F**), and nucleus basalis magnocellularis (Ch4; **G** and **H**). In A, ChAT-positive neurons are indicated by arrowheads whereas blood vessels are indicated by arrows. Photomicrographs D and F are inserts from C and E, respectively (delineated by the black rectangles). Scale bars are 250 μm in C and E; 60 μm in A,B,D,F, and G; and 6 μm in H.

ACKNOWLEDGMENTS

This work was supported by the Sandra Kolber Fund for Microvascular Surgery, Sir Mortimer B. Davis-Jewish General Hospital. H.M.S. is supported by grants from the Medical Research Council of Canada and the Fonds de la

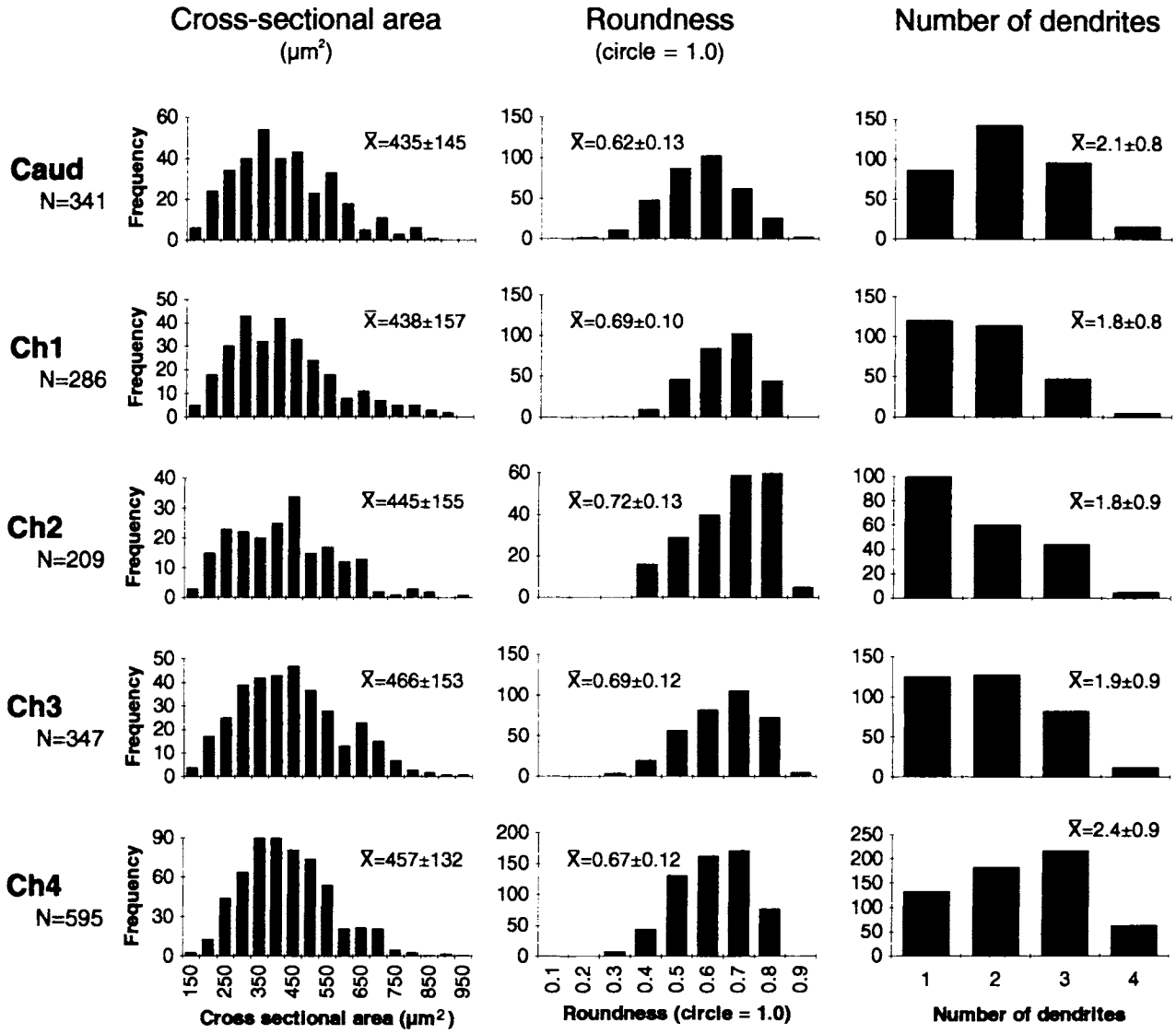

Fig. 4. Histograms of ChAT-positive neuronal profile sizes, cell roundness, and number of dendrites for five regions within the dog basal forebrain. N represents the number of ChAT-positive neurons sampled from four animals.

Recherche en Santé du Québec. This work was presented, in part, at the 29th Canadian Congress of Neurological Sciences in St-John's, June 27–30, 1994. The authors thank Mrs. Adrienne Liberman for excellent technical assistance.

LITERATURE CITED

Armstrong, D.M., C.B. Saper, A.I. Levey, B.H. Wainer, and R.D. Terry (1983) Distribution of cholinergic neruons in rat brain: Demonstrated by the immunocytochemical localization of choline acetyltransferase. J. Comp. Neurol. *216*:53–68.

Caplan, L.R., J.D. Schmahmann, C.S. Kase, E. Feldmann, G. Baquis, J.P. Greenberg, P.B. Gorelick, C. Helgason, and D.B. Hier (1990) Caudate infarcts. Arch. Neurol. *47*:133–143.

Funnell, W.R.J., D. Maysinger, and A.C. Cuello (1990) Three-dimensional reconstruction and quantitative evaluation of devascularizing cortical lesions in the rat. J. Neurosci. Methods *35*:147–156.

Garofalo, L., and A.C. Cuello (1994) Nerve growth factor and the monosialoganglioside GM1: Analogous and different *in vivo* effects on biochemical, morphological, and behavioral parameters of adult cortically lesioned rats. Exp. Neurol. *125*:195–217.

Gade, A. (1982) Amnesia after operations on aneurysms of the anterior communicating artery. Surg. Neurol. *18*:46–49.

Gorczyca, W., and G. Mohr (1987) Microvascular anatomy of Heubner's recurrent artery. Neurol. Res. *9*:259–264.

Gorry, J.D. (1963) Studies on the comparative anatomy of the gangion basale of Meynert. Acta Anat. *55*:51–104.

Larsson, C., J. Ronnberg, A. Forssell, L.-G. Nilsson, M. Lindberg, and K.-A. Angquist (1989) Verbal memory function after subarachnoid haemorrhage determined by the localisation of the ruptured aneurysm. Br. J. Neurosurg. *3*:549–560.

Lim, R.K.S., C.-N. Liu, and R.L. Moffitt (1960) A Stereotaxic Atlas of the Dog's Brain. Springfield, IL: Charles C. Thomas.

Mestre, N., and N. Bons (1993) Age-related cytological changes and neuronal loss in basal forebrain cholinergic neurons in *Microcebus murinus* (lemurian, primate). Neurodegeneration 2:25–32.

Mesulam, M.-M., E.J. Mufson, A.I. Levey, and B.H. Wainer (1983) Cholinergic innervation of cortex by the basal forebrain: Cytochemistry and cortical connections of the septal area, diagonal band nuclei, nucleus basalis (substantia innominata), and hypothalamus in the rhesus monkey. J. Comp. Neurol. *214:*170–197.

Mesulam, M.-M. (1991) Behavioral neuroanatomy of cholinergic innervation in the primate cerebral cortex. In R.T. Richardson (ed): Activation to Acquisition; Functional Aspects of the Basal Forebrain Cholinergic System. Boston: Birkhäuser, pp. 73–85.

Mesulam, M.-M., and C. Geula (1988) Nucleus basalis (Ch4) and cortical cholinergic innervation in the human brain: observation based on the distribution of acetylcholinesterase and choline acetyltransferase. J. Comp. Neurol. *275:*216–240.

Ries, F., R. Horn, J. Hillekamp, C. Honisch, M. König, and L. Solymosi (1993) Differentiation of multi-infarct and Alzheimer dementia by intracranial hemodynamic parameters. Stroke *24:*228–235.

St-Jacques, R., W. Gorczyca, P. Novak, and G. Mohr (1993) Microvascular anatomy of striate vessels in dogs: Contribution to an experimental model of forebrain ischemia. Can. J. Neurol. Sci. *20(Suppl.2):*S76.

Sweet, W.H., G.A. Talland, and H.T. Ballantine (1966) A memory and mood disorder associated with ruptured anterior communicating aneurysm. Trans. Am. Neurol. Assoc. *91:*346–348.

Talland, G.A., W.H. Sweet, and H.T. Ballantine (1967) Amnesic syndrome with anterior communicating artery aneurysm. J. Nerv. Mental Dis. *145:*179–192.

Vilkki, J. (1985) Amnesic syndromes after surgery of anterior communicating artery aneurysms. Cortex *21:*431–444.

Volpe, B., and W. Hirst (1983) Amnesia following the rupture and repair of an anterior communicating artery aneurysm. J. Neurol. Neurosurg. Psychiatry *46:*704–709.

West, M.J., L. Slomianka, and H.J.G. Gundersen (1991) Unbiased stereological estimation of the total number of neurons in the subdivisions of the rat hippocampus using the optical fractionator. Anat. Rec. *231:*482–497.

Yanagihara, T. (1991) Memory disorders in cerebral vascular diseases. In T. Yanagiharaand and R.C. Petersen (eds): Memory Disorders: Research and Clinical Practice. New York: Marcel Dekker Inc., pp. 197–225.